Magnetization analysis of oriented chains of hexagonal cobalt nanoplates

E. Vargas, J. C. Denardin, R. Lavín, P. Mascaró, C. Chaneac, and T. Coradin

Magnetization analysis of oriented chains of hexagonal cobalt nanoplates

E. Vargas,[1,2,3] J. C. Denardin,[1,2,a)] R. Lavín,[4] P. Mascaró,[1,2] C. Chaneac,[3] and T. Coradin[3]

[1]*Departamento de Física, Universidad de Santiago de Chile (USACH), Av. Ecuador 3493, Santiago 9170124, Chile*
[2]*Centro para el Desarrollo de la Nanociencia y Nanotecnología (CEDENNA), Av. Ecuador 3493, Santiago 9170124, Chile*
[3]*UMPC Univ Paris 06; CNRS, Chimie de la Matière Condensée de Paris, Collège de France, Paris 75005, France*
[4]*Facultad de Ingeniería, Universidad Diego Portales, Ejército 441, Santiago 8370191, Chile*

High quality single-crystalline hexagonal cobalt nanoplates have been obtained by a simple chemical reduction method using ultrasonic assistance. Individual nanoplates tend to form agglomerates due to their strong in-plane anisotropy. These particles were incorporated within a polyethylene matrix by a solution blending method and arrays of magnetic chains were generated by solidification of the solution of nanoparticles in the presence of a magnetic field. The easy axis of the Co plates is oriented along the field, in the direction of the chains length. Micromagnetic simulations, magnetic measurements, and FORC diagrams are used to clarify the complex magnetic behavior in these systems. © 2014 AIP Publishing LLC. [http://dx.doi.org/10.1063/1.4867345]

In recent years, controllable synthesis of low-dimensional metallic materials with special geometries has attracted interest due to their diverse potential applications in biomedicine and as novel material for engineering and electronic devices.[1] Nano and submicron-particles with high aspect ratio, particularly of Fe, Co, and Ni elements, have been studied because controlling the shape and morphology of particles is an effective method for tuning the magnetic properties.[2] In this line, several studies have focused on the simple and large-scale synthesis of regular and periodic magnetic structures.[3] Recently, there were various reports in the literature that describe the dispersion of ferromagnetic particles in polymeric matrices by in-situ polymerization, melt compounding and solution blending.[4–6] This latter method appears to be an attractive route because an external magnetic field provides the possibility of controlling the organization of the particles in the matrix.

In this work, large scale and high quality single-crystalline hexagonal cobalt nanoplates have been obtained by a simple chemical reduction method at room conditions without complex apparatus.[7] These particles were incorporated in a polyethylene matrix by a solution blending method. A complex structure formed by chains of spherical agglomerates of Co platelets forms spontaneously. The collective magnetic properties of this material have been studied by hysteresis loops and using first-order reversal curves (FORC) analysis.

Cobalt nanoplates were synthesized by our previous reported procedure.[7] In brief, 50 μl of cobalt chloride (0.4 M) and 15 ml of cetyltrimethylammonium bromide (4 mM) were mixed in typical glass vial on ultrasonic bath. Then, 100 μl of hydrazine was dropped in the reaction mixture and the pH was adjusted to 10 using ammonia solutions.

The final product was purified by magnetic decantation, washed several times, and dried. The morphological and structural characterization of the samples was carried out by scanning electron microscopy (SEM), in a Zeiss EVO MA10 and transmission electron microscopy (TEM), in a 120 kV Tecnai Spirit G2. The hysteresis loops was measured at room temperature on a vibrating sample magnetometer (VSM). The FORC curves were measured in a homemade Alternating Gradient Force Magnetometer (AGFM).

The nanocomposite film was produced by typical solution blending method under an external magnetic field of 2500 Oe.

Micromagnetic simulations were performed using the 3D OOMMF package.[8] Under this frame, the ferromagnetic system is divided into cubic cells with a uniform magnetization inside each cell. For our simulations, we use the typical Cobalt parameters: saturation magnetization $M_s = 1400 \times 103$ A/m, exchange stiffness constant $A = 30$ J/m, and a mesh size of 3 nm × 3 nm × 5 nm, where spins are free to rotate in three dimensions. In all the cases, the damping constant is 0.5.

Figure 1(a) shows the SEM image and reveals micron-long chains formed by the lineal organization of small particles. The magnified image (inset) shows particles with irregular shape and faceted surfaces, suggesting the existence of agglomerated nanoplates. To visualize details, a dilute colloidal solution was used to prepare TEM samples, as shown in Figure 1(b). This image shows perfect hexagonal particles. The size distribution was determined by processing 387 particles in several micrographs and has been adjusted by Gauss distribution, obtaining an average size about 300 nm. The inset of Figure 1(b) corresponds to the selected area electron diffraction (SAED) and shows the spots of mono crystalline hexagonal particle in 0001 hcp axis zone.

It was observed that the nanoparticles tend to agglomerate and to form long chains (see Figure 1(a)) due to their strong remanent magnetization and dipolar interactions. We generated nanocomposite films of Co nanoplates and polyethylene that were prepared in the presence of external field (oriented chains) and without field (not-oriented chains).

---

a)Author to whom correspondence should be addressed. Electronic mail: jcdenardin@gmail.com.
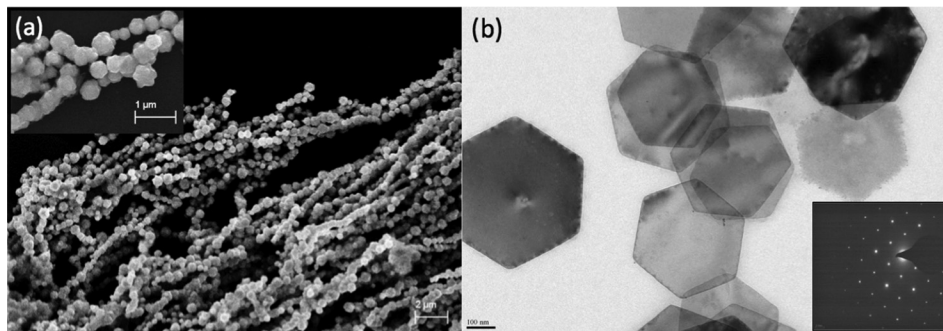
FIG. 1. (a) Panoramic and magnified SEM images of chains of agglomerated nanoplates. (b) TEM image and SAED pattern of the hexagonal nanoplates in hcp crystalline phase.
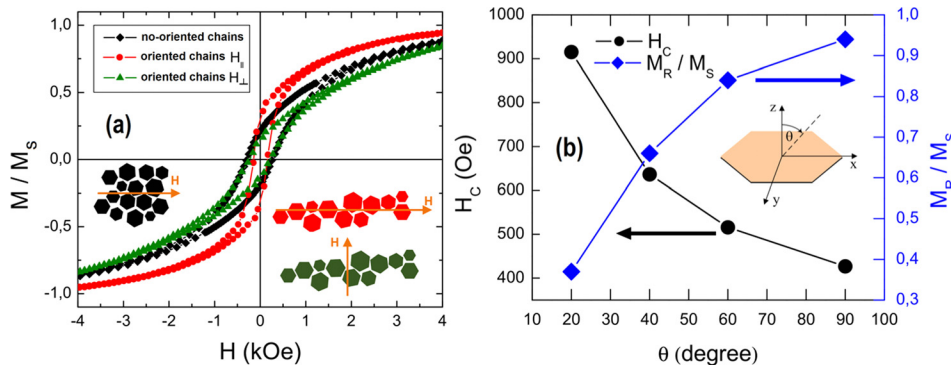

FIG. 2. (a) Magnetization curves normalized by M_s of Co chains in polymer, and measured as shown in the inset draws. (b) Coercivity and reduced remanence obtained from micromagnetic simulation of one hexagonal Co particle, as function of the angle θ between the external field and the z-axis (see the inset).

The magnetic properties of the samples were characterized with hysteresis loops as shown in Figure 2(a) for not-oriented chains and oriented chains with field. The samples that formed microchains were measured with the field parallel and perpendicular to the chains. From Figure 2(a), one can see that the disordered Co nanoplates (not-oriented chains) have a coercivity of 280 Oe and a remanent magnetization of 0.2. Figure 2(a) shows that there is a clear anisotropy, or easy magnetization axis, in the direction of the chains aligned by the external field. This means that it is easier to reach saturation when the field is applied in the direction of the chains than in the perpendicular direction. The coercivity values of the sample measured parallel and perpendicular to the chains are 150 Oe and 230 Oe, respectively.

In order to infer the magnetic behavior of these hexagonal nanoplates and how the arrays of nanoplates would tend to agglomerate, we have performed micromagnetic simulations, obtaining the coercivity and remanence of an isolated nanoplate with a diameter of 300 nm, with the magnetic field applied in different angles θ with the z-axis (the out of plane axis).

Figure 2(b) shows the coercivity and remanence from simulated curves as a function of angle θ between the z-axis and the external magnetic field. Because the easy axis is in the xy plane of the nanoplate, it is expected that when θ decreases the coercivity increases, as shown in Figure 2(b). One can see that the coercivity is strongly dependent on the out-of-plane orientation of the nanoplates with respect to the external magnetic field, varying from 306 to 915 Oe. The in-plane remanence of the nanoplate is more than two times higher than the out-of-plane remanence. This means that the individual nanoplates will tend to form agglomerates due to their strong in-plane remanent field, stacking individual hexagonal nanoplates to generate almost spherical agglomerates, as observed in the SEM image of Figure 1. When these agglomerates of

nanoplates are dried in presence of the magnetic field, their easy axis (the xy plane) will be oriented in the direction of the field, and consequently along the length of the chains, and the z-axis of the nanoplates can be oriented randomly in any direction perpendicular to the length of the chains.

In order to understand in more details the mechanism of magnetization reversal on these systems, we performed a more detailed magnetic analysis using the technique of FORC diagrams.[9–12] This technique is already being used to study different aspects of magnetic systems.[12–14]

Figure 3 shows the FORCs (a to c) and the corresponding diagrams (d to f) for the samples with not-oriented chains, and the oriented chains measured parallel and perpendicular to the field. The FORCs resemble the hysteresis curves of Figure 2 with the difference that now the complete internal area of the curves are filled with reversal curves. From Figure 3, it is worth noting that the FORCs for the not-oriented chains and the oriented chains measured in perpendicular direction do not present any visible difference (Figures 3(a) and 3(c)). On the other hand, the curve for oriented chains measured parallel is clearly different, being more vertical.

The diagrams of Figures 3(d)–3(f) show the distribution of coercivity fields (H_c) and interaction fields (H_i),[13,15] and allow one to perform a more detailed analysis of the magnetization reversal mechanisms that take place in these three configurations of the nanoplate arrays. The diagram for the not-oriented chains (Figure 3(d)) shows two distinct areas (sometimes called magnetic phases) that are more intense. One of this areas is centered at $H_c = 0$, that is attributed to the reversible magnetization contribution. This contribution is usually associated to the presence of a low coercivity reversible magnetic phase, and in this case could represent the contribution of the Co nanoplates that are in chains perpendicular to the field, or that have their hard axis (z plane) in
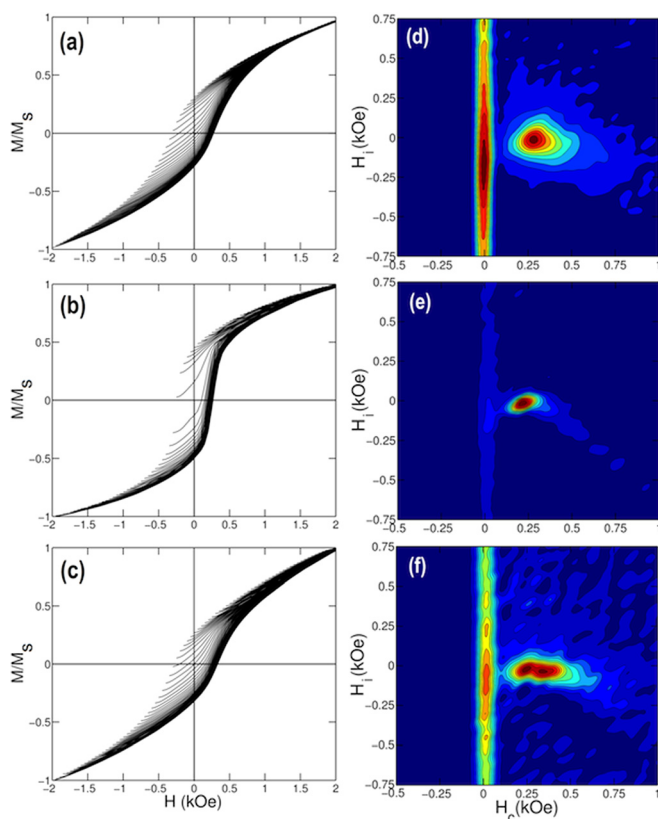
FIG. 3. FORCs measured for the three configurations: (a) not-oriented chains, (b) oriented chains with the external field parallel, and (c) perpendicular to the chains. The corresponding FORC diagrams for the three configurations are shown in (d to f).

the field direction. This reversible magnetization component can be observed in the FORC curves of Figure 3(a) as the positive slope at the beginning of each FORC curve.

The other region of the diagram is a small spot centered in $H_c = 0.28$ kOe, which represents the irreversible magnetic phase due to the nanoplates or arrays of nanoplates that reverse completely their magnetization with the external field, reaching a new equilibrium magnetization. One can also observe that this region presents a broad distribution of H_c, as a consequence of a distribution of nanoparticle size and/or a distribution of orientation of the nanoparticles with respect to the external field. The effect of interaction among the nanoparticles can be appreciated by the width of the distributions in the vertical axis, the H_i distribution.

The diagram obtained for the oriented chains measured parallel to the field (see Figure 3(e)) shows only one region of irreversible magnetization centered at $H_c = 0.25$ kOe. The size of this magnetic phase is smaller than in the disordered sample (Figure 3(d)), both in H_c and in H_i. As the physical size distribution of the nanoparticles is the same in both samples, this difference in the value of H_c distribution could be attributed to the smaller distribution of easy axis (xy planes) in the direction of the chains, as compared to the not-oriented sample. The fact that the reversible magnetic phase is not present is another indication of the bi-stability of the oriented chains generated by the external field in the sample preparation process.

When the oriented arrays of nanoparticles are measured in the perpendicular direction, the FORCs are very similar to the ones obtained for the disordered sample (see Figures 3(a) and 3(c)). However, the diagrams show distinct features, as shown in Figures 3(d) and 3(f). The main difference is the presence of two small spots superimposed in the main irreversible magnetic phase. The first spot is centered at the same H_c value of Figure 3(e), and the second spot spreads over a high field region, giving in average the same H_c distribution than in Figure 3(d). The H_i distribution is smaller than in Figure 3(d) and the reversible component appears again in this diagram, as a consequence of the fact that the z-axis of the nanoplates are oriented randomly in any direction perpendicular to the length of the chains.

From the previous results one can conclude that when the oriented chains are formed, very few nanoplates are oriented with their hard axis (z-axis) in the direction of the chains, resulting in a more vertical magnetization curve, with a small coercive field. When the magnetization curve is measured perpendicular to the chains, the magnetization reversal occurs through nanoplates that are oriented at different angles θ, increasing the coercivity of the system.

Based on the analysis of the different magnetic cooperative mechanisms, one can identify different magnetic entities that are present in the here-described Cobalt nanoplates systems. The simplest one is composed by the individual magnetic hexagonal Co platelets. The magnetic behavior of these individual hexagons cannot be observed by macroscopic measuring techniques as their strong magnetic anisotropy and aspect ratio induce their agglomeration in almost spherical particles. The more complex structure is the chain of spherical agglomerates that also forms spontaneously but whose direction can be controlled by solidification of the solution of nanoparticles in the presence of magnetic field in a polymer. The easy axis of the Co stacks is oriented along the field, in the direction of the chains length. Micromagnetic simulations and the careful analysis of the magnetization curves and the FORC diagrams are particularly useful to investigate the collective magnetic properties of these systems.

[1]D. V. Talapin *et al.*, Chem. Rev. **110**, 389–458 (2010).
[2]R. Xu *et al.*, Cryst. Growth Des. **7**, 1904–1911 (2007).
[3]S. Behrens, Nanoscale **3**, 877–892 (2011).
[4]Q. He *et al.*, Polymer **53**, 3642–3652 (2012).
[5]T. Wen and K. M. Krishnan, J. Phys. D: Appl. Phys. **44**, 393001 (2011).
[6]D. Younesi *et al.*, Mater. Des. **43**, 549–559 (2013).
[7]E. Vargas *et al.*, Mater. Lett. **94**, 121–123 (2013).
[8]M. J. Donahue and D. G. Porter, OOMMF User's Guide, Version 1.2a3 2002, http://math.nist.gov/oommf.
[9]C. R. Pike *et al.*, J. Appl. Phys. **85**, 6660–6667 (1999).
[10]C. R. Pike, Phys. Rev. B **68**, 104424 (2003).
[11]R. Lavín *et al.*, J. Magn. Magn. Mater. **324**, 1800–1803 (2012).
[12]R. K. Dumas *et al.*, Phys. Rev. B **75**, 134405 (2007).
[13]R. Lavín *et al.*, IEEE Trans. Magn. **44**, 2808–2811 (2008).
[14]H. Chiriac *et al.*, J. Magn. Magn. Mater. **316**, 177–180 (2007).
[15]G. Bertotti, *Hysteresis in Magnetism* (Academic Press, NY, USA, 1998).